Supplemental Figure S1; Related to Figure 1

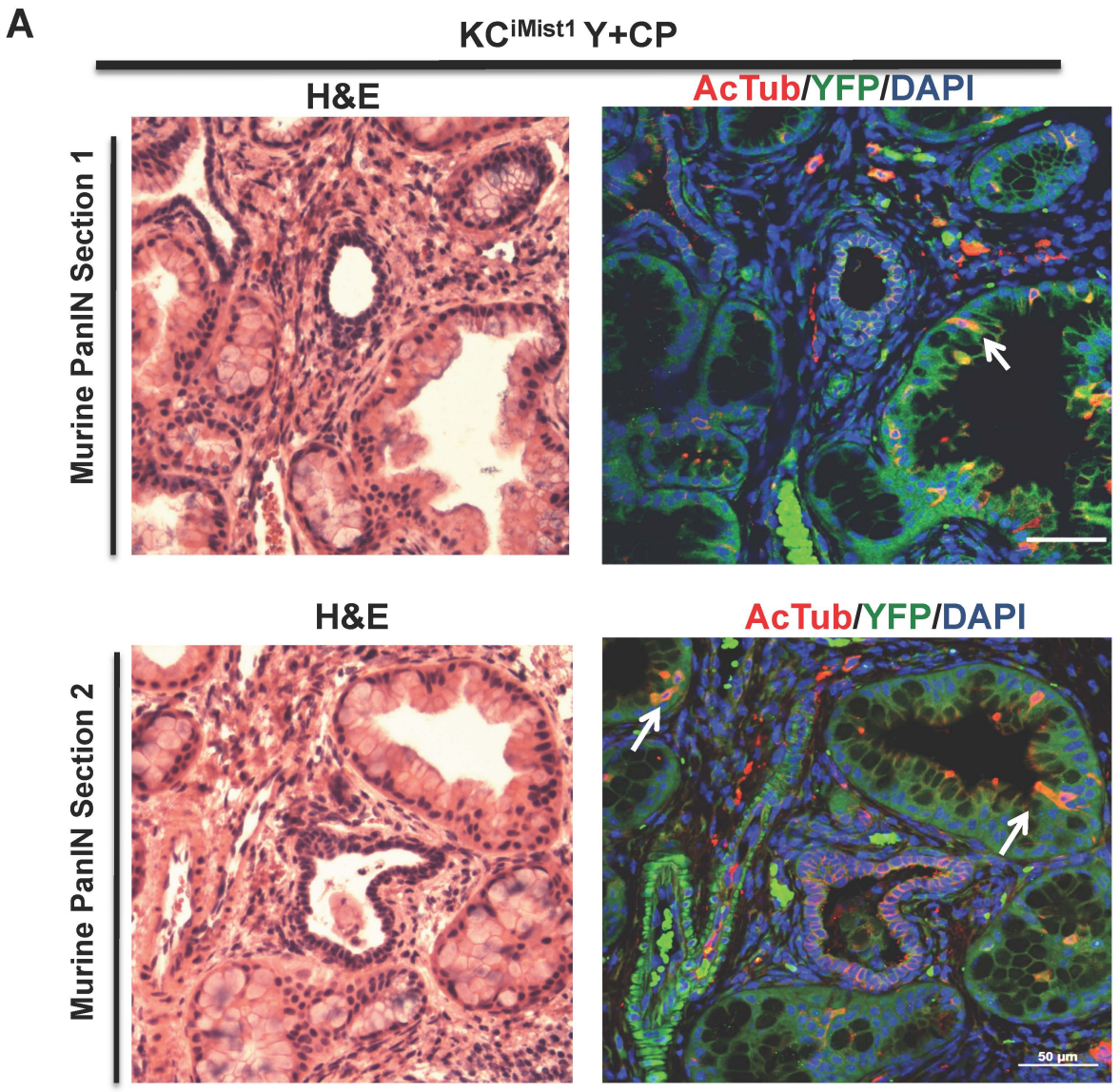

Figure S1. Lineage tracing experiments in confirm acinar cell origin of AcTub+ cells in murine PanIN. KC^{iMist1} mice were bred onto the Rosa26:LsL-*YFP* Cre reporter background (Y), thereby generating KC^{iMist1}Y mice. PanIN formation was further accelerated by the induction chronic pancreatitis (CP). **(A)** H&E analysis of murine PanIN sections and corresponding immunoflourescent labeling with AcTub and YFP. Arrows show representative AcTub+ cells marked by YFP lineage label.

Supplemental Figure S2; Related to Figure 2

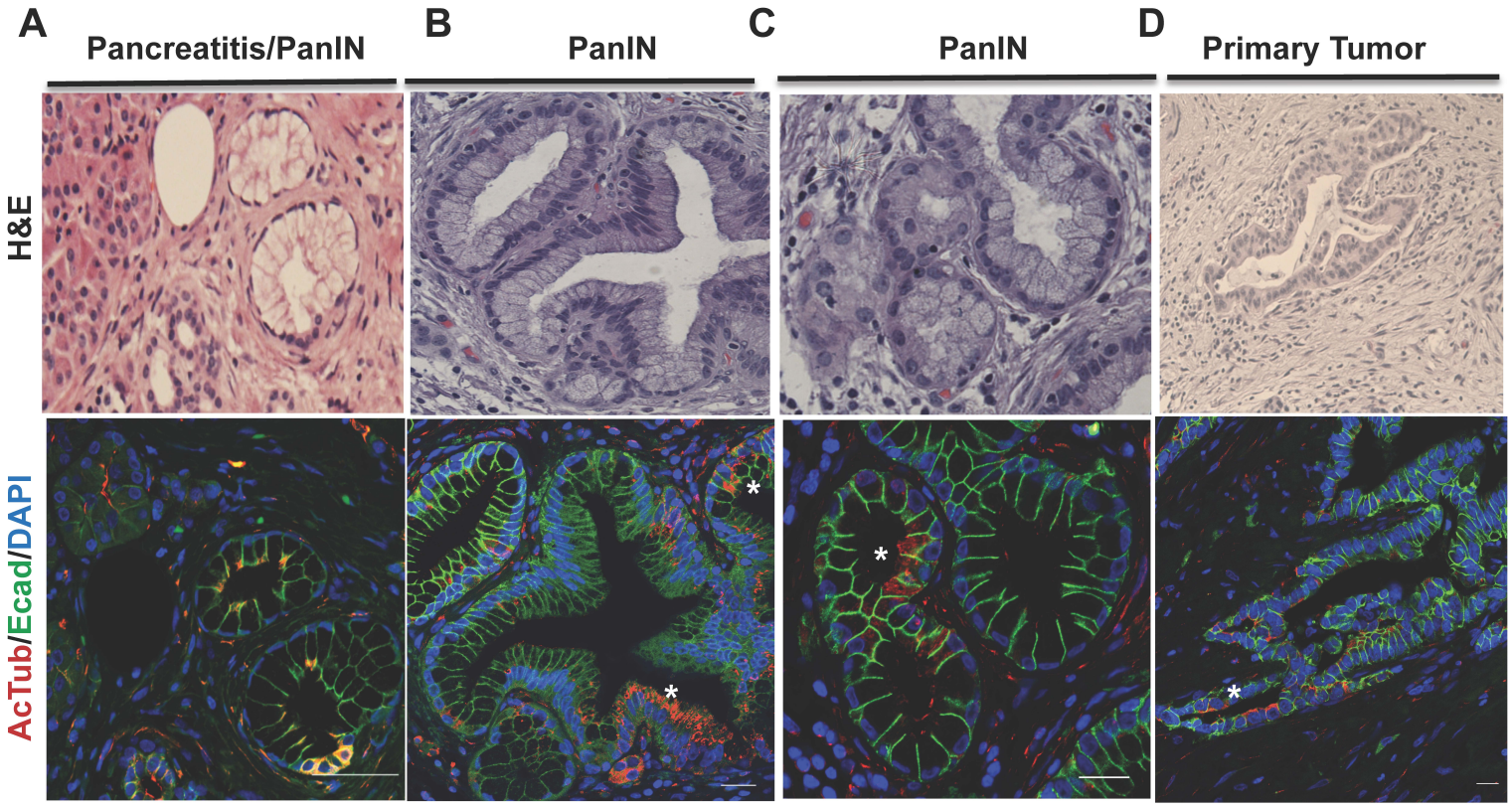

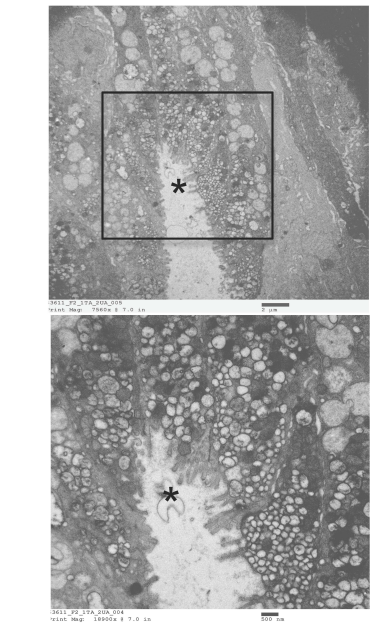

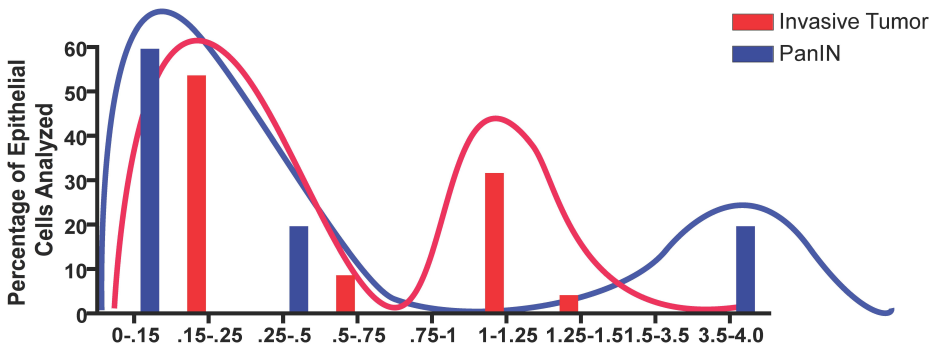

Figure S2. Immunoflourescent analysis of AcTub in human pancreatic cancer and bimodal distribution of maximal microvillus length in murine PanIN and human pancreatic cancer.

(A-D) H&E and immunoflourescent labeling of AcTub (red) and Ecadherin (green) in human pancreatitis, PanIN and and PDAC tissues. Cells with high levels of cytoplasmic and apical AcTub are denoted by (*). **(E)** Transmission electron micrograph of cells that exhibi tapical microvilli in human invasive pancreatic tumors. The black box outlines representative tumor cells exhibiting microvilli greater than 1.0μM in length. **(F)** Quantification of maximal microvillus length in murine PanIN and human invasive pancreatic cancer. Note that in both cases there is a bimodal distribution in microvillus length, suggesting a subpopulation of cells with distinct morphology.

Supplemental Figure S3; Related to Figures 4 & 5

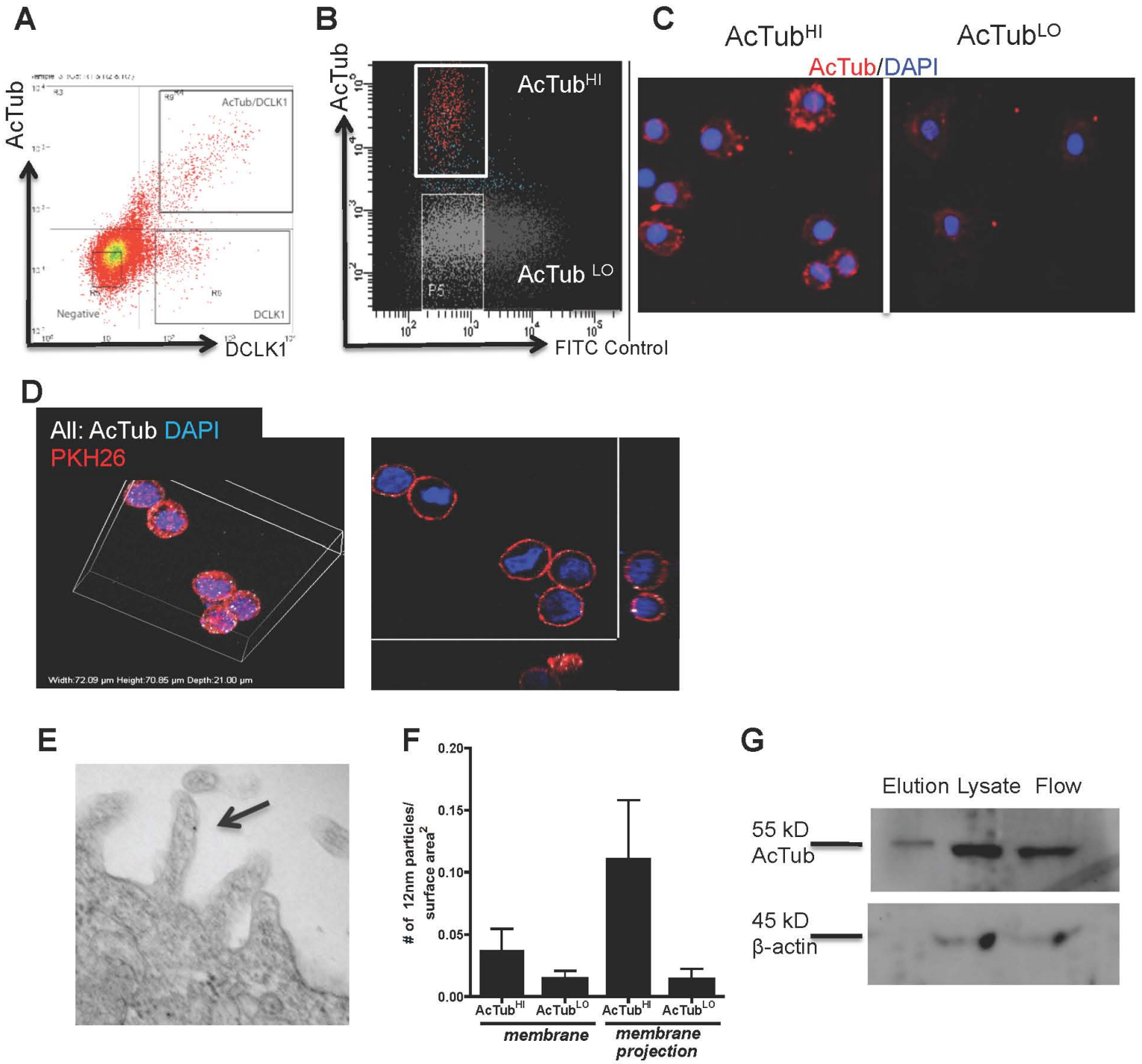

Figure S3. AcTub epitopes are detectable on the cell surface. (A) FACS plot showing greater than 90% overlap between AcTub labeling and DCLK1. A small percentage (<20%) of DCLK1^{HI} cells do not label positive for AcTub. **(B)** Representative cell surface labeling with AcTub antibody. **(C)** FACS sort followed by cytospin, fixation and labeling for AcTub. Cells with isolated based on cell surface AcTub express higher levels of cytoplasmic AcTub. **(D)** Live (unfixed) cell labeling and confocal imaging of CFPAC cells. PKH26 (red) stains the cell membrane. Left image shows maximal intensity projection of Z-stack images. Right image shows single optical section. Note punctate labeling of AcTub on cell surface. **(E)** Transmission electron micrograph of FACS-sorted AcTub^{HI} cell. Arrow points to immunogold labeling for AcTub on a membrane projection. **(F)** Quantification of the number of 12nm gold particles on either the membrane or membrane projection in FACS-sorted AcTub^{HI} vs AcTub^{LO} cells. **(G)** Cell surface biotinylation experiment documents the presence of AcTub in the eluted fraction, further validating the presence of AcTub on cell surface.

Supplemental Figure S4; Related to Figure 5

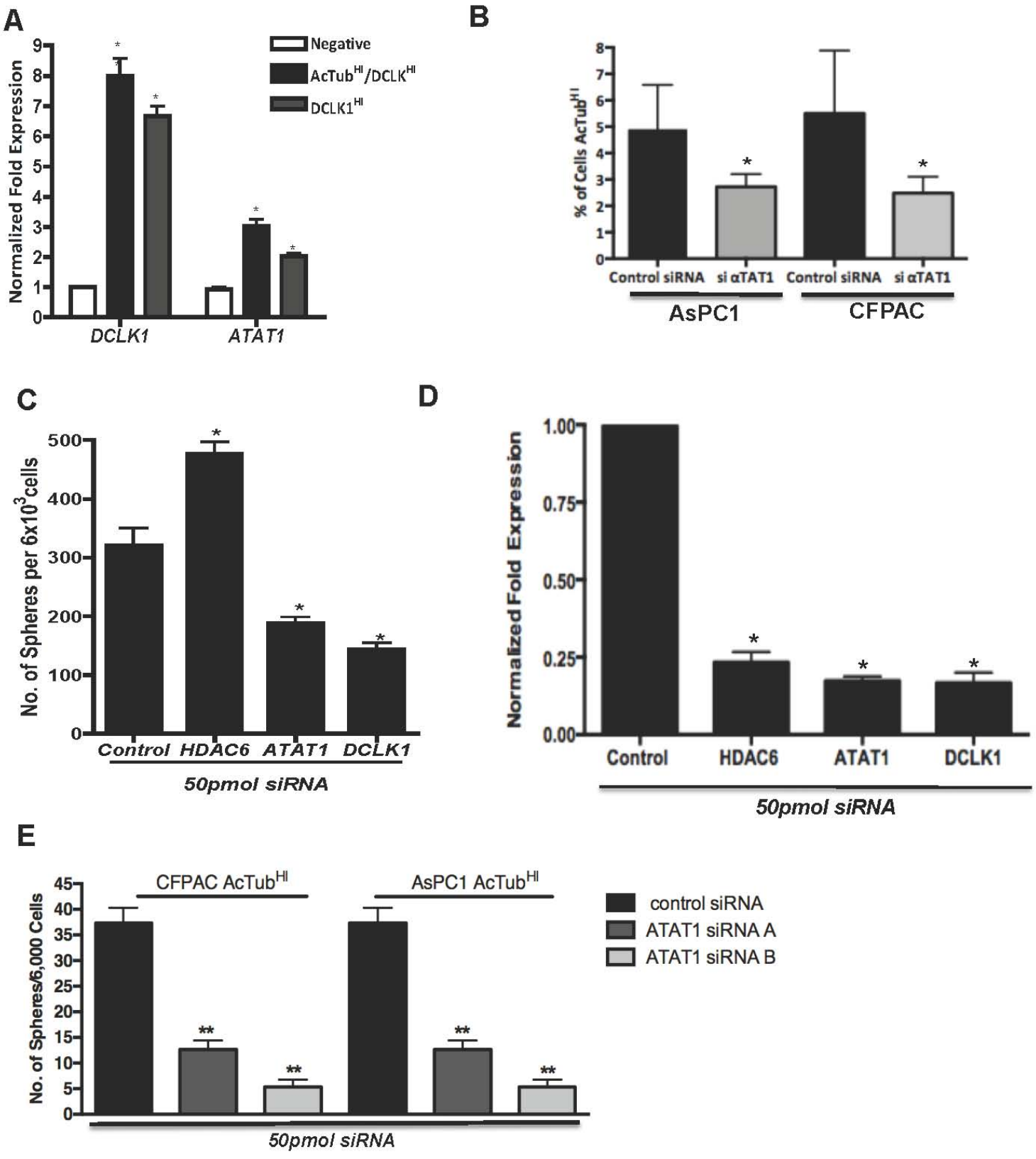

Figure S4. AcTub^{HI}/DCLK1^{HI} PDAC stem cell function is regulated by tubulin acetylation and DCLK1. (**A**) Quantitative Real Time PCR confirming increased expression of *DCLK1* and *ATAT1* in FACS sorted AcTub^{HI}/DCLK1^{HI} cells. (**B**) siRNA mediated knockdown of *ATAT1* in AsPC1 cells decreases cell surface labeling of AcTub by 50% (*p<0.05). (**C**) siRNA mediated knockdown of *ATAT1* in FACS sorted AcTub^{HI} cells significantly decreases their sphere forming capacity (**p<0.01). (**C**) siRNA mediated knockdown of target genes regulates the sphere forming ability of CFPAC human pancreatic cancer cells (**p<0.01). (**D**) Quantitative RT-PCR to confirm the siRNA-mediated knockdown of HDAC6, DCLK1 and ATAT1 mRNA *in vitro*. (**E**) Knockdown of ATAT1 and DCLK1 significantly decreases sphere forming ability while knockdown of HDAC6 significantly increases sphere forming ability (*p<0.05).

Supplemental Figure S5; Related to Figure 5

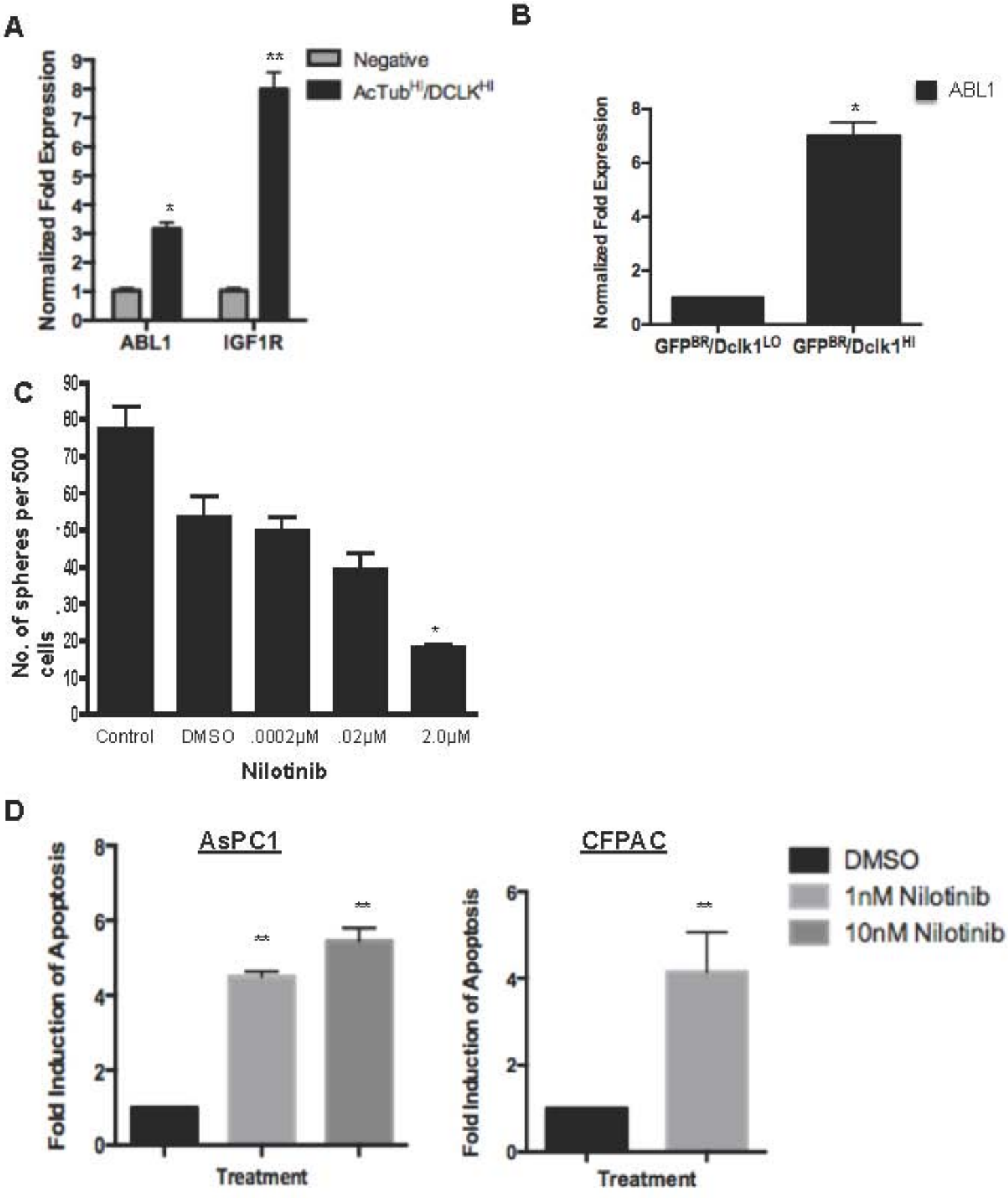

Figure S5. AcTub^{HI}/DCLK1^{HI} PDAC stem cell function is regulated by ABL1. **(A)** *ABL1* and *IGF1R* mRNA were both more highly expressed in FACS sorted AcTub^{HI}/DCLK1^{HI} cells relative to AcTub^{LO}/DCLK1^{LO} cells (**p<0.01, *p<0.05). **(B)** *ABL1* is more highly expressed in GFP^{Br}/Dclk1^{HI}cells than GFP^{Br}/Dclk1^{LO} cells(*p<0.05). **(C)** Quantification of the number of spheres formed from the CFPAC cell line after treatment with Nilotinib. Treatment of CFPAC spheres with Nilotinib (ABL inhibitor) significantly decreases the number and size of spheres (**p<0.01). Sphere reduction was mediated by an induction of apoptosis, as assessed by PI labeling (**D**).

II. Supplemental Methods

Mouse Procedures

LsL-Kras^{G12D} (Tuveson et al., 2004), Mist1CreERT2 (Habbe et al., 2008), R26R^{YFP} (Srinivas et al., 2001), mTmG (Muzumdar et al., 2007) and Pdx1 (Gannon et al., 2000) mice have been described previously. For KC^{iMist1} and KC^{Pdx1} experiments, non-Kras expressing littermates were consistently used as controls. The KC^{iMist1} mice were breed to both the R26R^{YFP} and mTmG backgrounds to assess for recombination and fate mapping of recombined cells. Recombination of the LsL-Kras^{G12D} allele was deteted using the primers listed on the following site: http://web.mit.edu/jacks-lab/protocols/KrasCond_tablesTWO.html.

Tamoxifen (Sigma) was dissolved in corn oil and administered intraperitoneal (IP) at a dosage of 5mg per injection. This dosage was given for three consecutive days. Mice that received caerulein (Peptide) were injected at a dosage of 50ug/kg diluted in sterile 1XPBS. Mice were given this dosage three times a week for three weeks and the three dosages were given in one-hour intervals.

siRNA Constructs and Experiments For the transient knockdown of ATAT1, HDAC6 and DCLK1, smartpool siRNA constructs were purchased from Santa Cruz or Dharmacon. Reverse transfection experiments were performed using Lipofectamine RNAiMax. 50pmol of siRNA were transfected in 6-well low attachment plates. For AcTub specific experiments, 6x10^3 AcTub^{HI} cells were sorted per well. For experiments using bulk cancer cell line populations, the cells were trypsinized, counted and seeded at 6x10^3 cells per well. Spheres were counted 96 hours after transfection and RNA was isolated from spheres to confirm mRNA levels of the siRNA targets were decreased.

Xenograft Experiments

We used one human low-passage xenograft that was a surgical specimen obtained from a pancreatic cancer patient. The dissociation of xenograft tumors and subsequent xenograft experiments were performed as described previously(Rasheed et al.).

Quantitative RT-PCR Analysis

FACS sorted mouse pancreatic cells or human pancreatic cell lines were sorted into RLT buffer containing Beta mercaptoethanol. RNA was extracted using the Qiagen RNeasy mini kit and columns. cDNA was generated using the Qiagen one step RT-PCR handbook. Quantitative RT-PCR was done using Sybr Green (company). The following probes were used for RT-PCR: DCLK1 (human) Forward: AGT CTT CCG ATT CCG AGT TGA G; Reverse: CAG CAA CCA GGA ATG TAT TGG A; Dclk1 (mouse) Forward: CAG CCT GGA CGA GCT GGT GG; Reverse: TGA CCA GTT GGG CTT CAC AT. ß-actin Forward: GGT GAT CCA CAT CTG CTG CAA; Reverse: ATC ATT GCT CCT CCT CAG GG; Hes1 Forward: ACG TGC GAG GGC GTT AAT AC; Reverse: GGG GTA GGT CAT GGC ATT GA; Hey1 Forward: ATC TGC TAA GCT AGA AAA AGC CG; Reverse: GTG CGC GTC AAA GTA ACC T; ATAT1 Forward: GGC GAG AAC TCT TCC AGT AT; Reverse: TTG TTC ACC TGT GGG ACT; HDAC6 (obtained from santa cruz with siRNA knockdown construct), IGF1R Forward: AGGATATTGGGCTTTACAACCTG Reverse: GAGGTAACAGAGGTCAGCATTTT and ABL: Forward: TGAAAAGCTCCGGGTCTTAGG; Reverse: TTGACTGGCGTGATGTAGTTG.

Flow Cytometry, Cell Sorting and Colony Formation

Mouse Pancreas

Cells were sorted from two different sources: (1) mouse pancreas tissue and (2) human pancreatic cancer cell lines. Mouse pancreatic tissue was digested with collagenase and processed for antibody staining as described previously (Rovira et al.). After being

processed, primary antibodies Acetylated alpha tubulin (Sigma) and DCLK1 (abcam) were incubated on ice for one hour. The cells were then washed with 1XPBS and secondary antibodies were used (Jackson) alexa-fluor 647 anti-rabbit or alexa-fluor 647 anti-mouse. For sorting experiments, control mouse pancreas served as the initial gating of cells, based on forward and side scatter properties. The next set of cells was from untreated mTmG dissociated pancreas, which served as a fluorescent control for each experiment. This was used to appropriately calibrate the red fluorescence. Tamoxifen-treated C^{iMist1} or KC^{iMist1} mice were then used to locate the GFP+ fraction. Secondary antibody only controls were used for antibody staining and dead cells were excluded using Propidium Iodide (2μg/ml). For sphere forming experiments, the cells were sorted into FBS (Gibco) then seeded into 96 well low attachment plates using media and conditions described previously (Rovira et al.).

Human Pancreatic Cancer Cell Lines

For FACS sorting human pancreatic cancer cell lines, the cells were first trypsinized then treated briefly with FBS containing media. The cells were pelleted and washed with 1XPBS three times before the cells were incubated with primary antibodies (AcTub) or DCLK1 (abcam) CD44 (BD Biosciences), CD24 (BD Biosciences), ESA (BD Biosciences), CD133 (abcam). Antibodies were allowed to incubate on ice for one hour and the cells were washed then treated with secondary antibodies, unless the primary antibodies were directly conjugated. For the ALDEFLUOR reaction (Stem Cell Technologies, Vancouver, CA), the cells were diluted in ALDEFLUOR reaction buffer at a concentration of $1x10^6$ cells per ml. Control tubes contained both ALDEFLUOR reagent (5μl) and the inhibitor diethylamino-benzaldehyde (DEAB) 10μl. Another set of tubes contained ALDEFLOUR alone (5μl). The reactions were allowed to incubate in a 37°C incubator for 30 minutes. To set up the gates for FACS, one tube was used as a

control that had no ALDEFLOUR or antibody staining. Another tube contained either secondary antibody staining alone or ALDEFLUOR+DEAB to set the gates for nonspecific staining. Dead cells were excluded with PI. Cells were sorted into sterile FBS before being cultured in 6 well low-attachment plates in DMEM or methylcellulose containing media supplemented with FBS and Pen-Strep as described previously (Rasheed et al.).

Transmission Electron Microscopy (TEM)

Samples were fixed in 2.5% glutaraldehyde, 3mM $CaCl_2$, 1% sucrose, in 0.1 M sodium cacodylate buffer, pH 7.2 for one hour at room temperature. After buffer rinse, samples were postfixed in 1% osmium tetroxide in buffer (1 hr) on ice in the dark. Following a DH_2O rinse, plates were stained with 2% aqueous uranyl acetate (0.22 µm filtered, 1 hr, dark) , dehydrated in a graded series of ethanol and embedded in Eponate 12 (Ted Pella) resin. Samples were polymerized at 60^{o}C overnight.

Thin sections, 60 to 90 nm, were cut with a diamond knife on the Reichert-Jung Ultracut E ultramicrotome and picked up with naked 200 mesh copper grids. Grids were stained with 2% uranyl acetate in 50% methanol and observed with a Hitachi 7600 TEM at 80 kV. Images were captured with an AMT CCD (1K x 1K) camera.

Immuno-Electron Microscopy (IEM)

Samples were fixed in 4% paraformaldehyde (freshly prepared from EM grade prill form), 0.2% glutaraldehyde, 3mM $MgCl_2$, 1% sucrose in 0.1 M phosphate buffer, pH 7.2 for at least 15 minutes at 4^{o}C. After buffer rinse, samples were stained in 0.12% tannic acid (0.5 hr), followed by a buffer rinse, and 0.5 hr in ammonium chloride. Following a buffer rinse in 0.1 M maleate and 3% sucrose, pH 6.2, samples were stained with 2% aqueous uranyl acetate (0.22 µm filtered, 0.5 hr, dark) and dehydrated in a

graded series of ethanol before embedding in LR-White (Ted Pella) resin. Samples were polymerized at 50^{o}C overnight.

Thin sections, 60 to 90 nm, were cut with a diamond knife on the Reichert-Jung Ultracut E ultramicrotome and picked up with formvar coated nickel grids, 2x1 mm. Grids were labeled with primary antibody overnight, followed by secondary antibody for 1 hour and observed with a Philips CM120 TEM at 80 kV. Images were captured with an Orius CCD (1K x 1K) camera.

Immunohistochemistry and Histology

Mouse pancreata were fixed overnight in 4% paraformaldehyde and embedded in paraffin. Paraffin-embedded tissue was cut serially into 5μM-thick sections. For analysis of histology, hematoxylin and eosin staining was done. Slides were carefully reviewed by J.M.B. and A.M. on an Olympus BX40 light microscope and images were acquired using a Nikon Digital Sight Camera.

Immunoflourescence (IF)

Paraffin-embedded blocks were sectioned and deparaffinized in xylene then hydrated in Ethanol. After antigen retrieval (Vector), the tissue was permeabilized with 1.0% PBST and primary antibodies were incubated overnight at 4°. Primary antibodies include acetyled α tubulin (Sigma), DCLK1 (abcam), Ecadherin (BD Biosciences) and GFP (Invitrogen). After washes with 1xPBS, secondary antibodies were incubated at room temperature for 1 hour, nuclei were stained with DAPI and the cells were mounted using immunoflourescent mounting medium (DAKO). Images were captured using a NikonA1 confocal microscope.

Microarray

$AcTub^{HI}$ and $AcTub^{LO}$ cells were FACS sorted and RNA was isolated using the Qiagen RNeasy Isolation Kit. RNA samples were then submitted for analysis of a Whole Genome Microarray Kit, 4x44K (Agilent).

Sample preparation for 3-dimensional imaging

Mice were transcardialy perfused by 4% paraformaldehyde for fixation. Afterwards, pancreases were harvested and were post-fixed in 4% paraformaldehyde solution for 1 hour at 25°C. The fixed tissues were permeabilized with 2% Triton X-100 solution at 4°C overnight. Before the staining steps, the tissues were incubated with the blocking buffer (2% Triton X-100, 10% normal goat serum, and 0.02% sodium azide in PBS). Then the primary antibody, monoclonal rabbit anti-mouse DCLK1 (Epitomics, Burlingame, CA), was diluted (1:50) in the dilution buffer (0.25% Triton X-100, 1% normal goat serum, and 0.02% sodium azide in PBS) and incubated overnight at 15°C. Alexa fluor 647 conjugated goat anti-rabbit secondary antibody (1:200, Invitrogen) was used to reveal the immunostained structure. The nuclei were counter stained by propidium iodide (25 μg/mL, Invitrogen) at room temperature for 1 hour. The labeled specimens were immersed in the optical-clearing solution FocusClear (CelExplorer, Hsinchu, Taiwan) (Fu et al., 2009; Fu and Tang) overnight before being imaged via confocal microscopy. The images were obtained by the Zeiss LSM 710NLO-Meta multiphoton microscope which equipped with a 40× LD "C-Apochromat" water immersion objective lens (Carl Zeiss, Jena, Germany). Afterwards, the voxel-based confocal micrographs were processed with Avizo 7.1 image reconstruction software (VSG, Burlington, MA).

III. Supplemental References

Fu, Y. Y., Lin, C. W., Enikolopov, G., Sibley, E., Chiang, A. S., and Tang, S. C. (2009). Microtome-free 3-dimensional confocal imaging method for visualization of mouse intestine with subcellular-level resolution. Gastroenterology *137*, 453-465.

Fu, Y. Y., and Tang, S. C. At the movies: 3-dimensional technology and gastrointestinal histology. Gastroenterology *139*, 1100-1105, 1105 e1101.

Rasheed, Z. A., Yang, J., Wang, Q., Kowalski, J., Freed, I., Murter, C., Hong, S. M., Koorstra, J. B., Rajeshkumar, N. V., He, X.*, et al.* Prognostic significance of tumorigenic cells with mesenchymal features in pancreatic adenocarcinoma. J Natl Cancer Inst *102*, 340-351.

Rovira, M., Scott, S. G., Liss, A. S., Jensen, J., Thayer, S. P., and Leach, S. D. Isolation and characterization of centroacinar/terminal ductal progenitor cells in adult mouse pancreas. Proc Natl Acad Sci U S A *107*, 75-80.